Lawrence Berkeley National Laboratory

Recent Work

Title

Return flows from beaver ponds enhance floodplain-to-river metals exchange in alluvial mountain catchments.

Permalink

https://escholarship.org/uc/item/9ft6b7xq

Authors

Briggs, Martin A
Wang, Chen
Day-Lewis, Frederick D
et al.

Publication Date

2019-10-01

DOI

10.1016/j.scitotenv.2019.05.371

Peer reviewed

eScholarship.org Powered by the California Digital Library
University of California

Return flows from beaver ponds enhance floodplain-to-river metals exchange in alluvial mountain catchments

Martin A. Briggs[1*], mbriggs@usgs.gov

Chen Wang[2]

Frederick D. Day-Lewis[1]

Ken Williams[3,4]

Wenming Dong[3]

John W. Lane[1]

[1]U.S. Geological Survey, Earth System Processes Division, Hydrogeophysics Branch, 11 Sherman Place, Unit 5015, Storrs, CT USA

[2]Department of Earth and Environmental Sciences, Rutgers University, Newark, NJ USA

[3]Lawrence Berkeley National Laboratory, Earth & Environmental Sciences Area, 1 Cyclotron, Road, MS74R316C, Berkeley, CA USA

[4] Rocky Mountain Biological Lab, Gothic, CO USA

Abstract

River to floodplain hydrologic connectivity is strongly enhanced by beaver-(*Castor canadensis*) engineered channel water diversions. The hydroecological impacts are wide ranging and generally positive, however, the hydrogeochemical characteristics of beaver-induced flowpaths have not been thoroughly examined. Using a suite of complementary ground- and drone-based heat tracing and remote sensing methodology we characterized the physical template of beaver-induced floodplain exchange for two alluvial mountain streams near Crested Butte, Colorado, USA. A flowpath-oriented perspective to water quality sampling allowed characterization of the chemical evolution of channel water diverted through floodplain beaver ponds and ultimately back to the channel in 'beaver pond return flows'. Return seepages were universally suboxic, while ponds and surface return flows showed a range of oxygen concentration due to in-situ photosynthesis and atmospheric mixing. Median concentrations of reduced metals: manganese (Mn), iron (Fe), aluminum (Al), and arsenic (As) were substantially higher along beaver-induced flowpaths than in geologically controlled seepages and upstream main channel locations. The areal footprint of reduced return flow seepage flowpaths were imaged with surface electromagnetic methods, indicating extensive zones of high-conductivity

shallow groundwater flowing back toward the main channels and emerging at relatively warm bank seepage zones observed with infrared. Multiple-depth redox dynamics within one focused seepage zones showed coupled variation over time, likely driven by observed changes in seepage rate that may be driven by pond stage. High-resolution times series of dissolved Mn and Fe collected downstream of the beaver-impacted reaches indicated seasonal dynamics in mixed river metal concentrations. Al time series concentrations showed proportional change to Fe at the smaller stream location, indicating chemically reduced flowpaths were sourcing Al to the channel. Overall our results indicated beaver-induced floodplain exchanges create important, and perhaps dominant, transport pathways for floodplain metals by expanding chemically-reduced zones paired with strong advective exchange.

Key words: river; groundwater/surface water interactions; beaver; floodplain; drone; water quality

1. Introduction

The concept of ‘river corridor’ science recognizes that the quality of flowing surface waters is intrinsically linked to their contributing catchments through hydrologic connectivity, including lower terrestrial hillslopes, floodplains, and riparian zones (Covino, 2017; Poole, 2010; Vidon et al., 2010). Bidirectional river-floodplain exchange in particular can be critical to basin water storage and nutrient transformation dynamics (Harvey and Gooseff, 2015), yet floodplain hydrologic exchange flows are often driven primarily by episodic high-flow events (e.g. Sawyer et al., 2014) or relatively slow-exchanging, long hyporheic flowpaths (Boano et al., 2014). Beaver (*Castor canadensis*) disrupt these abiotic floodplain exchange drivers by actively diverting large quantities of channel water laterally using an engineered series of dams, impacting both wet and dry season floodplain connection (Westbrook et al., 2006). As humans allow beaver to return to their extensive natural habitats across North America, the fundamental dynamics of river corridor hydrologic connectivity are being strongly altered toward a template of spatial ‘discontinuum’ and enhanced exchange (Burchsted et al., 2010). Much beaver-induced floodplain disturbance is undoubtedly viewed as a net positive in the context of natural and efficient watershed restoration. But as beaver ponds and seepage zones accompanying beaver activity often exhibit suboxic to hypoxic conditions (Collen and Gibson, 2000), there is the potential to mobilize large quantities

of reduced metals and associated contaminants from alluvial sediments to streams and rivers.

Beaver populations are steadily increasing in North America due to stricter trapping laws, a general decline in trapping interest, passive and active conservation efforts, and a relative absence of predators (Hood, 2011). In one sense, this rebound can be viewed as North American watersheds returning to a natural, or pre-European settlement state one that is extensively engineered by the beaver. Before European settlement the North American beaver population numbered between 60-400 million individuals (Seton, 1929), and their dams and foraging influenced almost every floodplain system from arid Mexico to the arctic tundra (Naiman et al., 1988). After the arrival of significant numbers of Europeans in the early 1600's beaver populations declined in response to extreme trapping until the animal was functionally extinct on the continent by 1900. Before trapping began, most rivers in North America had extensive beaver-induced floodplains and numerous wood snags that retained carbon and nutrients in the headwaters. Evidence of the extensive effects on the riparian landscape of large historical populations can still be seen hundreds of years later (Naiman et al., 1986).

Beaver construct dams across streams and wetlands to increase habitat favorable to their basic needs of forage and protection. Impoundments can have a variety of influences on the physical and

biological characteristics of floodplain areas and riparian zones. Analogous to anthropogenic dams, the combined effects of beaver dams is often a reduction in peak river discharge, a smoothing of catchment outlet hydrograph (Ligon et al., 1995), and a general increase in reach-scale water residence time (Jin et al., 2009). These moderated flow patterns can stabilize the stream channel and decrease bed mobilization by reducing erosive forces, such as shear stress on the stream bank and along the sediment-water interface. Storage of water behind the dams can be an appreciable fraction of the catchment surficial water budget during dry periods and often results in greater connection between riparian vegetation and the water table throughout the year. An analysis of aerial photo mosaics from 1948 to 2002 from Central Alberta, Canada indicated that the number of ‘active’ beaver lodges could explain greater than 80% of the variability in floodplain open water area through a number of wet and dry periods (Hood and Bayley, 2008). However, the beaver-induced water storage story is complex. Some studies have also suggested that the ecological effects of increased water storage may be negated in part by amplification of the evaporative flux due to an increase in stream and floodplain surface water area (Collen and Gibson, 2000). Recent work has indicated that beaver-induced recharge of alluvial floodplains may not substantially increase late summer low-flows, in part because much of this floodplain water may be trapped in low permeability soils and/or is simply recently diverted channel water (Nash et al., 2018). However, flows returning to the channel from reactive beaver-

induced floodplain storage are likely to be important conduits of carbon transport (Catalán et al., 2017) and nutrient transformation (Briggs et al., 2013; Wegener et al., 2017) throughout the year.

The recent phenomena of encouraging beaver recolonization and the installation of anthropogenic ‘beaver dam analogues’ in the context of stream restoration hopes to capitalize on expected net positive hydrogeological and ecosystem impacts (Lautz et al., 2018; Pilliod et al., 2018; Wohl et al., 2015). Natural and simulated dams can mitigate incised western channels by increasing floodplain connection and riparian vegetation regrowth, which in turn positively influences desirable recreational fish populations (Bouwes et al., 2016). The channel water temperature response to beaver-induced floodplain connection is complicated and spatially heterogeneous (Majerova et al., 2015), but it has been shown to moderate the warmest daily temperatures and provide cool thermal refugia for stressed aquatic species in Oregon (Weber et al., 2017). Benefits of beaver colonization that may outweigh complications to infrastructure have even been recently recognized for urban drainages (Bailey et al., 2019). However, not all impacts of natural and simulated beaver dams will be desirable to humans (Pilliod et al., 2018). Negative impacts of result mainly from the raising of the water table adjacent to the stream, flooding, impoundment of drainage systems, and the cutting of desirable vegetation (Collen and Gibson, 2000).

Gradients in pH and redox conditions along chemical pathways between riparian soils and stream sediments are also strongly affected by beaver impoundment. For example, in some systems oxic soils move/regress farther away from the original channel as the water level rises, and the magnitude of anoxic soil area grows accordingly (Naiman et al., 1988). Anoxic conditions can readily develop on the floodplain due to the tranquil flow regime of beaver ponds and large supply of local organic carbon, and along biogeochemically reactive subsurface flowpaths that route floodplain water back to the channel, creating ‘natural reduced zones’ (NRZs, e.g. Dwivedi et al., 2018). Anoxic soils may increase the acid neutralizing capacity of the soil water due to the retention of nitrate and sulfate, and act as a net source of iron and ammonium ions (Cirmo and Driscoll, 1993), though quantitative research regarding beaver-induced mobilization of reduced chemical species is generally lacking. Microbial activity of floodplains and riparian zones has been found to be greatly increased by impoundments, a process that has important implications from the pore- to the landscape-scale (Wegener et al., 2017). Enhanced biogeochemical reactivity and potential mobilization of floodplain nutrients, metals, and contaminants necessitates a more complete understanding as beavers are increasingly regarded as a stream restoration solution. Recent studies have signaled beaver-related stream restoration practices may be outpacing fundamental science regarding the wide ranging physical and chemical impacts of such projects (Lautz et al., 2018; Pilliod et al., 2018).

For river corridor hydrologic exchanges to be influential to water quality, hydrologic exchange flows need to be both chemically reactive and of appreciable volume compared to river discharge so as to alter net channel solute transport dynamics (Wondzell, 2011). While biogeochemically reactive cross-meander bend hyporheic exchange may be prevalent in most alluvial river corridors, a combination of relatively low hydraulic gradient and tight floodplain soils can limit the impact of this exchange on net river chemistry (Pai et al., 2017), particularly at the km-reach scale. In contrast, beaver dams are known to push large volumes of surface water laterally into the floodplain through engineered fill and spill pathways. Here, we characterize the natural metal transformation and transport dynamics of a specific type of river corridor hydrologic exchange flow, termed here: ‘beaver pond return flows.’ Like the more well-known ‘irrigation return flows’ to rivers driven by the application of water to adjacent cropland (Essaid and Caldwell, 2017), beaver pond return flows are enabled by the purposeful redirection of water outside of the channel. Redirected channel water that is not lost to floodplain evapotranspiration returns to the river in a spectrum of surface flows and subsurface seepage zones (Majerova et al., 2015). By using a combination of remote sensing and direct contact measurements, we identify beaver-induced floodplain exchange flowpaths along two two alluvial mountain streams of varied size. Chemical measurements collected across a full-year hydrological cycle (neglecting winter months) at the pond return flows, and at other observed groundwater seepage types, indicate beaver-induced

floodplain exchange can be a dominant mechanism of natural metals flux along alluvial river corridors. Further, extensive deposition of solid metal oxides at return flow discharge points likely provides an important source/sink function for a variety of contaminant transport problems. The evidence to support these statements is shown in the following sections.

2. Materials and Methods

A suite of complementary ground- and drone-based heat tracing and remote sensing methodology was used to characterize the hydrogeological template of beaver-induced floodplain exchange for two alluvial mountain streams of disparate size. A flowpath-oriented perspective to water quality sampling allowed characterization of the chemical evolution of channel water diverted through floodplain ponds and ultimately returned to the channel.

2.1 Study Area

The Lawrence Berkeley National Laboratory Watershed Function Scientific Focus Area (SFA) has established an experimental watershed encompassing the drainages of the East River near Crested Butte, Colorado (USA) to quantify the myriad nested processes impacting the ability of mountainous systems to retain and release water, nutrients, carbon, and metals. This scientific ‘community watershed’ hosts ongoing research spanning a wide range of spatial scales and physical, chemical, and biological processes. The SFA encompasses the drainages of the East River, Washington Gulch, Slate River (including Oh-Be-Joyful Creek), and Coal Creek

(Figure 1a). Although each watershed has analogous sections of meandering alluvial stream, they also display unique flow dynamics, current land use practices, and legacies of mining-related contamination. While there is some direct impact from cattle ranching along the East River corridor, that system is generally considered a ‘pristine’ end-member due to the lack of substantial mining activity and ore-rich rock draining its environs. In contrast, Coal Creek and the Slate River are more highly influenced by heavy metals, such as arsenic, copper, cadmium, and zinc due to legacy mine activities in those drainages. For the focus areas of the current study, we chose analogous, meandering open valley sections of the larger East River and smaller Coal Creek with observed contemporary beaver inhabitation (Figure 1a). This research began as broader investigation of natural metal mobility and metal oxide deposition at geologically-controlled groundwater seepages throughout the SFA; however, early in the study, it became apparent that beaver pond return flows were likely to be an important metals flux pathway to consider, and the research plan was adapted accordingly.

2.2 Aerial mapping of floodplain beaver ponds

Floodplain zones inundated with beaver-induced exchange of channel water are difficult to navigate on the ground, but the typical open canopy nature of such areas presents opportunity for small unoccupied aerial vehicle (sUAS, or ‘drone’) and satellite-based mapping techniques. We deployed various multirotor sUAS (3D Robotics Solo, 3D Robotics, Berkeley, CA) at the East River reach from August 12-17, 2017 and July 28-August 2, 2018; and at

Coal Creek on July, 31 2018. During sequential flights the sUAS were equipped with various sensors, similar to the approach described by Briggs et al., (2018). For high-resolution visible imagery we used a Ricoh GRII Camera (Ricoh Imaging Company, Ltd., Japan). Image stills from multiple flight lines, altitudes (generally 200-350 ft above ground surface), and directions were compiled into larger “stitched,” georectified orthoimages of the river corridor using Agisoft PhotoScan software. Position of the aircraft was tracked by internal GPS, and although ground control points were deployed for some flights, they were not used in postprocessing of the visible imagery. Structure from motion (SfM) techniques were then applied using Agisoft PhotoScan software to generate time-specific surface digital elevation models of floodplain structure and exposed channel geomorphology. Details regarding the UAS sensor specifications and the calculated spatial precision of the compiled orthoimages are listed in the public data release of this data at Briggs et al., (2019b). Although the imagery from satellites is of substantially lower resolution than that achievable with sUAS, there may be an existing wealth of historical imagery available to assess longer term beaver pond structure dynamics. We used Google Earth (Google, Mountain View, CA, USA) to qualitatively assess beaver occupation of the Coal Creek reach back to 1999 (earliest available clear imagery).

2.3 Geolocation and characterization of seepage zones

Thermal infrared is sensitive to the water surface 'skin' temperature (Handcock et al., 2006) and can be used to geolocate river corridor seepage zones and identify surface water flow patterns at times of natural thermal contrast (Dugdale, 2016; Hare et al., 2015). We expected discharge of deeper groundwater to approximate the surface annual mean temperature (approximately 8°C, Constantz, 2008) whereas shallow groundwater discharge and pond return flows should be warmer in summer, providing multiple characteristic targets for infrared imaging. Thermal infrared data were collected on the ground using handheld FLIR i7 and T600bx series cameras (FLIR Systems, Wilsonville, OR) throughout the beaver-impacted reaches and along an additional approximate 6 km of the upper East River and within the nearby Oh-Be-Joyful Creek drainage. The purpose of the larger-scale thermal infrared mapping was to identify a range of dominant non-beaver-impacted groundwater discharge (seepage) zones for geochemical characterization. To augment the ground-based thermal surveys throughout the beaver-impacted floodplain areas we collected radiometric thermal infrared data from sUAS using a gimbal-mounted FLIR VUE Pro R 13mm camera.

Because thermal infrared imaging may not reliably locate submerged seepage zones, particularly in fast flowing rivers (Hare et al., 2015), armored fiber-optic distributed temperature sensing (FO-DTS) cables were deployed along an approximate 2.4 km floodplain channel length at the East River

from August 15 to August 22, 2017. FO-DTS technology for environmental temperature sensing is thoroughly reviewed by Tyler et al., (2009). Effort was made to emplace the weighted cables along the sediment-water interface of the ‘cutting’ banks of meander bends as these locations typically show enhanced exchange of surface and groundwater. FO-DTS data were collected with a Sensornet Oryx control unit (Sensornet Ltd., United Kingdom) run in double-ended mode at 10-min acquisition time per channel (20-min per measurement) and 1.01 m linear spatial resolution.

Once seepage zones of various type were identified, stream flow was physically gauged for several of the higher volume discharges using small custom surface weirs, graduated cylinders, and a stopwatch. Slow flowing ‘diffuse’ seepage rates were evaluated at 4 discrete locations along an East River side channel margin, down gradient of a large beaver pond, where seepage was indicated by thermal imaging and Fe-oxide staining from August 23 to November 4, 2017. For comparison, seepage was also monitored over this period within an adjacent spatially focused, higher flow beaver pond return seepage zone. Vertical seepage rates were tracked over time using profiles of shallow (0.01, 0.07, 0.11 m depth below sediment-water interface) saturated sediment temperatures collected with iButton thermal data loggers (Maxim Integrated DS1922L) run at 0.0625 °C precision embedded in short steel pipes, as described in detail by Briggs et al. (2014). The workflow suggested by Irvine et al., (2017) that combines diurnal temperature signal-based thermal parameter measurements with diurnal

signal amplitude attenuation was used to perform the analytical modeling of vertical water flux rates. The fundamental (diurnal) sinusoids were derived from the raw temperature data using the Captain Toolbox (Young et al., 2010) and VFLUX2 (Irvine et al., 2015) Matlab-based programs. Vertical flux was evaluated over time with the amplitude ratio-based analytical models of VFLUX2, a site-specific thermal diffusivity estimated from vertical diurnal temperature signal transport (e.g. Luce et al., 2013), and an estimated sediment porosity of 0.5 (fine floodplain sediments).

2.4 Water quality monitoring and sampling

Two types of water chemistry data were collected: 1. spatially-distributed synoptics covering seepage zones, off-channel ponded areas, and main channel locations, and 2. main channel high-resolution time series over years 2017-18. Synoptic water samples were collected using 60 mL plastic Luer-Lok syringes and filtered through single-use Millex 0.45-µm Luer-Lok filters. There were four synoptic sampling events in total: 1. August 19-22, 2017; 2. June 21-22, 2018; 3. July 29-August 3, 2018; and 4. September 23-25, 2018, with the largest suite of samples collected during event 3, and a subset of sample locations visited during other events. Sample water was stored in 125 or 250 mL polypropylene bottles, preserved with 2-ml trace metal grade HNO_3, and kept in an ice cooler or refrigerated until evaluated for dissolved Fe, Mn, As, and Al by either the U.S. Geological Survey Water Quality Laboratory or the University of Connecticut Center for Environmental Sciences & Engineering Laboratory. Main channel chemical time series of Fe,

Mn, and Al were collected by grab sample every few days from spring into the fall of 2017 and 2018. Time series sample collection locations were approximately 1 km downstream of the Coal Creek and East River beaver-impacted floodplain zones. Stream water samples were collected daily to weekly depending upon snow and ice conditions using an automatic water sampler (Model 3700; Teledyne ISCO, NE, USA), with samples pumped via peristaltic pump into uncapped 1 L polyethylene bottles. Sample bottles were retrieved at regular intervals, with 25 mL aliquots filtered (Pall, NY, USA; PTFE; 0.45 µm) and preserved with trace metal grade 12 N HNO_3 until analysis. Cation and trace metal concentrations were determined using ion coupled plasma mass spectrometry (ICP-MS) (Element 2, Thermo Fisher, MA, USA).

Field parameters (dissolved oxygen (DO), specific conductivity at 25 °C (SpC), and temperature) were typically evaluated at the time of synoptic water sample collection with a SmarTroll MP handheld sensor (In-Situ Inc., United States). DO was also tracked over time in summer 2018 in two of the larger East River floodplain ponds using MiniDOT loggers (Precision Measurement Engineering, Inc., Vista, CA, USA) paired with electrical conductivity/pressure loggers (Solinst Levelogger Junior Edge, Solinst Canada Ltd, Ontario, CAN). To investigate temporal redox dynamics of beaver return flow seepage, a vertical profile of redox potential (Eh) was also collected (surface pool, 0.05, 0.1, 0.15, 0.2, 0.25 m depths) at the same focused return

flow seep mentioned above from June 22 to July 13, 2018 using a custom designed logging (1 min increments) redox probe (Paleo Terra, Netherlands).

Although thermal infrared is useful for locating surface seepage locations, the geometry of the flowpaths that feed those seepage zones, and their connection to upgradient water sources, is typically inferred. However, near-surface electrical geophysical methods can be used to map flowpaths of reduced groundwater, as various redox processes release ions into solution increasing the bulk electrical conductivity (EC) of the subsurface (Binley et al., 2015). We used a hand carried electromagnetic induction GEM-2 frequency-domain instrument (Geophex, Ltd.) to evaluate bulk conductivity of the near surface. Data were collected in the vicinity the East River return flow seeps instrumented with iButton sensors on September 23, 2018 and throughout the Coal Creek beaver-inhabited floodplain corridor on September 25, 2018. The GEM2 tool was operated over 7 frequencies ranging 1,530-93,090 Hz and the expected depth of investigation limit was approximately 5 m. Similar to the groundwater/surface water exchange study of Ong et al. (2010) we did not invert the data but instead work with apparent bulk electrical conductivity (EC) , which was estimated from raw (e.g. not smoothed) quadrature data using EMInvertor software (Geophex, Ltd.) based on the GEM-2 instrument coil separation (1.66 m).

3. Results and Discussion

A combination of drone-based imaging and ground-based heat tracing, geochemical and geophysical measurements indicated beaver-induced floodplain exchanges create important, and perhaps dominant, transport pathways of natural metals. All data presented below are publicly available from Briggs et al., (2019b, 2019a) and Williams et al., (2019).

3.1 Spatial dynamics of geologic seeps and beaver pond return flows

Numerous types of beaver dams, ponds, and return flows were observed along the East River and Coal Creek study reaches, some of which are shown Figure 1b-e. Heat tracing was used to identify spatially preferential channel/floodplain and groundwater connectivity via thermal infrared and FO-DTS technology. Specifically, riverbed interface temperature was recorded with FO-DTS over 6 days in August 2017 along the main East River channel adjacent to the ponded floodplain. Mean temperature along the cables generally ranged from 10.0 to 10.6 °C (full diel range of approximately 8 °C or less), showing subtle warming with downstream distance over the 2.5 km beaver impacted reach (Figure 2). No strong cold anomalies approximating deeper groundwater (approximately 7-9 °C) temperature were observed, indicating discharge of deeper flowpaths to the river is likely not an important process of hydrologic exchange along beaver-impacted section of floodplain. This finding is consistent with the FO-DTS-based hydrogeological characterization of Pai et al. (2017) for a meandering reach immediately downstream of our study reach. Although there are

several steep, 10’s of m high cutbanks into the shale bedrock along the reach that might be expected to produce groundwater seepage (Winter et al., 1998), shale is typically of low permeability and no substantial groundwater discharge was observed from the outcrops over two summer field seasons. A few discrete valley wall seepages were located visually/with infrared, and groundwater discharge from these was captured by beaver ponds before entering the river, as discussed below.

Several discrete warm temperature sections are notable in the mean FO-DTS record (Figure 2). During retrieval of the FO-DTS cable, we found that approximately 6 of these warm anomalies resulted from new beaver dam shunts that had been built since the cable was deployed, of the type depicted in Figure 1b. These locations are also indicated by large temperature standard deviation anomalies, as the cable was exposed in part to dynamic air daily temperatures. These high variance zones are spatially coupled with slightly cool, less variant temperatures where the cable was buried inside the dam materials (Figure 2). The fortuitous real time observations of shunt dam building shows channel water diverting structures can be built by beaver in just a few days, altering river/floodplain connectivity in a substantial and sustained way. Two additional discrete sections of FO-DTS cable showed paired warm mean temperatures and low standard deviation (‘R’ in Figure 2). These are interpreted (and field confirmed with bed temperature probing) as return flow seepage zones, as strong upwelling of even relatively warm water is expected to buffer riverbed

interface temperature. Both return flow seepage locations were located adjacent to major floodplain beaver impoundments. Our FO-DTS results show that return flow seepages can be of high enough magnitude to measurably alter sediment-water interface temperature in the main channel of larger, fast flowing rivers where heat tracing methods are typically challenged to locate zones of exchange.

Thermal infrared surveys conducted throughout the East River beaver reach in summer 2017 and 2018 showed that the floodplain ponds were typically warmer than the main channel by afternoon, and that beaver pond return flows can be identified as warm anomalies (e.g. Figure 3C), as indicated by FO-DTS. In contrast one small beaver pond along the steep valley wall of Coal Creek was entirely sourced by a large hillslope spring of presumably deeper groundwater (Figure 1d). This spring water was colder than the main channel (Figure 3d), demonstrating that not all return flows will contribute to warming of channel water in summer, which agrees with the finding of Weber et al., (2017) that beavers can enhance thermal heterogeneity (cold and warm) in some systems. However, the larger ponded areas along Coal Creek floodplain away from the valley wall contained relatively warm, diverted channel water, similar to the East River floodplain. A more spatially extensive thermal infrared survey conducted along the upper East River corridor where the valley is much narrower and steeper, and along the bedrock lined, steep Oh-be-Joyful Creek, identified dozens of cold groundwater discharges emanating directly from fractured bedrock. A

443subset of these ‘geologic’ seeps were sampled for chemical comparison to
444the beaver pond return flows, as described in Section 3.2 below.

445 Visual imagery collected by sUAS was integrated to build high
446resolution orthomosaics of the East River (Figure 4) and Coal Creek (Figure
4475) beaver reaches. Surface digital elevation models were also derived from
448the visual imagery and used to infer floodplain surface flow patterns based
449on elevation changes (Supplemental Figures A1, A2). Although not
450attempted for this study, such structure-from-motion drone imaging products
451are likely to be useful for ‘fill and spill’ numerical flow modeling of ponded
452areas. The 2017 East River orthomosaic demonstrates the extensive
453saturated floodplain area induced by beaver-induced shunting of channel
454water (Figure 4a, b). It appeared that just 2 shunts placed at strategic
455locations, namely at the confluence of a river oxbow and along a river side
456channel, were responsible for the majority of diverted channel water over
457both summer seasons (Figure 4 a). These shunts were less effective in
458July/August 2018 due to a lower flow condition causing widespread draining
459of the floodplain ponded areas (Figure 4c), though the floodplain morphology
460appeared comparable to 2017. A rain event the day before the 2017 sUAS
461mapping mobilized fine sediments and the resulting turbidity was used as a
462natural qualitative tracer of advective flow connectivity through the linked
463ponded systems (Figure 4b). These flow patterns indicate preferential
464pathways through more stagnant ponded areas.

The pond systems generally terminated near a large meander bend of the river, where clusters of beaver pond return seeps transferred water back to the channel (Figure 4b, c). No prominent surface return flows were noted in summer 2017 or 2018 along the East River floodplain section. However, a survey in later September 2018 showed that at the lowest channel flow condition beaver were able to build several spanning dams across the East River, diverting more water into the floodplain, refilling and overflowing the ponded areas and creating numerous overland return flows. It may be that alluvial mountain rivers of similar large size to the East River go through a natural beaver diversion cycle: 1. Large spring snow melt pulses damage or destroy the previous year's dam structures (also shown by Briggs et al., (2013)); 2. In early summer river discharge recedes but river stage is still relatively high and shunts are effective to divert water to the floodplain, but channel-spanning dams cannot yet be constructed (Figure 1b);. 3. In mid-summer, channel flow drops farther (typically by a factor of 10x from spring peak at the East River, i.e. USGS gage 09112500) and the shunts are less-effective but channel spanning dams cannot yet be built, causing a recession of floodplain pond levels (Figure 4c); 4. At the lowest flows in early fall, spanning dams are built, refilling the ponded areas before winter. Longer term, higher-frequency monitoring is needed to explore these temporal dynamics. In contrast to the East River, channel spanning dams were observed along the Coal Creek system across 2017 and 2018 summer and early fall seasons (Figure 5a). Remarkably, each of four successive dams

temporarily diverted almost the entirety of channel flow into the adjacent floodplain in 2018 (Figure 5a, c, d), and this diverted water returned to the downstream channel in a series of surface and subsurface return flows. Discharge from two of the larger surface return flows was measured at 173 and 346 m3/d (with mobile weirs) in August 2018, representing a large input of sub-oxic water back to the main channel. Extensive Fe-oxide staining was visible along the floodplain ponded areas (rust colors, Figure 5c), but oxide deposition was not associated with the smaller groundwater spring-fed beaver pond. A downstream ponded floodplain area captured another groundwater discharge originating from a road culvert on the hillslope above the floodplain (Figure 5d), and this oxic groundwater mixed with reduced floodplain water before entering the channel in a series of subsurface seepages. Beaver dam capture of discrete hillslope groundwater discharge was also noted at multiple locations along the East River, indicating that floodplain ponds should be considered in groundwater/surface water exchange studies that are typically focused on hyporheic exchange alone. Google Earth imagery from 1999, 2005, and 2012 of the Coal Creek reach showed similar (to 2018) floodplainpond morphology and the existence of channel spanning dams diverting large portions of streamflow (Supplemental Figure A3), indicating ‘disturbance’ caused by beaver inhabitation may create a relatively stable new floodplain exchange dynamic.

3.2 Dissolved chemistry of beaver-induced floodplain exchanges and geologic seeps

Earlier work has indicated the potential for beaver impoundments to expand zones of reducing conditions in saturated soils (Cirmo and Driscoll, 1993; Naiman et al., 1988). Recently, NRZs have been identified in other Colorado floodplain systems as key locations of nutrient transformation (Boye et al., 2017; Dwivedi et al., 2018) and contaminant accumulation (Janot et al., 2016). However, although NRZs have strong, spatially compressed redox gradients, they are not all likely to function as hotspots of reaction influential to the larger floodplain system chemistry, or ecosystem 'control points.' Reducing conditions can develop locally due to enhanced organic carbon availability and/or residence time (Boano et al., 2010), but spatially-compressed redox gradient alone does not indicate mass flux of reduced chemical species. To influence mixed river water metals concentrations, NRZs must also have appreciable advective exchange with the channel. Our sUAS-based surface mapping and return flow observations indicate beaver-induced flowpaths may dominate river-floodplain advective flux compared to other types of lateral exchange in these systems (Figure 7a), but a more quantitative picture is developed with chemical analysis.

Synoptic chemical samples were collected at a combination of main channel (29 samples), beaver pond (14 samples), beaver pond return flow (17 samples), and geologic seep (14 samples) locations; although all parameters (DO, SpC, Mn, Fe, Al, As) were not always evaluated for each

sample. Although floodplain ponds were relatively easy to physically access, sample filters clogged quickly there, practically limiting pond sample numbers. Spot measurements at the time of water sample collection showed return flows had the lowest median DO concentration at 47% saturation (Figure 6a). However, overall return flows ranged from fully anoxic to fully saturated in DO. This large range can be explained by return flows being comprised of both surface and subsurface flowpaths, with the latter generally of considerably lower DO saturation. Surprisingly, most pond samples were super-saturated in DO, owing to abundant observed primary production (filamentous algae) in the shallow open pools, as all samples were taken during daytime hours. The temporal records from the two major East River floodplain beaver ponds show a more complete story, with large swings from daytime DO super saturation (e.g. >11 mg/L DO diurnal swings) to nearly anoxic conditions overnight, suggesting a system with strong continual aerobic respiration (Figure 7b). Elevation-corrected DO saturation was estimated with the Benson and Krause Equations (US Geological Survey, 2011). Oxygen is the master variable that controls redox condition (Zarnetske et al., 2012), so strong daytime photosynthesis signal of beaver ponds can impart a highly dynamic redox signal onto return flowpaths that are otherwise suboxic. The DO time series data indicate that our daytime pond grab samples for dissolved metals may underestimate daily average levels, as night time suboxic conditions would be expected to enhance metal concentrations. As the 2018 summer progressed, the pond became suboxic

though extensive pond algae was still observed (Figure 7b), so it is possible net aerobic respiration increased during this period, and/or advective circulation of the ponds decreased at lower water levels.

The SpC of beaver pond return flows showed the largest median conductivity at 351.0 µS/cm, with the high end of that range driven by seepages (Figure 6b). This result indicated the potential for subsurface return flow pathways to be mapped with electromagnetic imaging due to enhanced bulk EC, as described below. Ponds showed the largest total range as SpC driven in part by pre-sampling precipitation events and mixing with valley wall groundwater discharges. Other types of measured groundwater discharge, predominantly from fractured bedrock, also showed a large range in SpC but the lowest median value at 158.8 µS/cm.

Beaver-induced flows were most distinct from other river corridor water sample types in respect to dissolved concentrations of Fe and Mn (Figure 6 c,d; Figure 7c). Return flows averaged (median) 1120.0 and 210.6 µg/L for Fe and Mn, respectively, with the maximum Fe value of 14,260.0 µg/L collected in August 2017 at the major East River return flow seepage instrumented with a redox profiler. For contrast, the median Fe and Mn concentrations (µg/L) in the other three types of samples are: channel (169.1 Fe /4.7 Mn), beaver ponds (366.8 Fe / 19.2 Mn) and geologically controlled groundwater (54.9 Fe / 1.3 Mn). As floodplain beaver pond water is dominated by channel diversions, with some discrete hillslope groundwater

inflow, metal concentrations are clearly increased by beaver-induced hydrologic exchanges.

While it is not uncommon to find high concentrations of natural metals in reduced floodplain soil porewater (Schulz-Zunkel and Krueger, 2009), what makes beaver pond return flows unique is that they also show strong advective flux. Hyporheic exchanges in larger river systems often may not substantially impact mixed river solute transport, particularly at the reach-scale (Wondzell, 2011). However, in the East River system dissolved Mn concentrations collected in 4 surveys over a year always increased in mixed main channel water along the beaver-impacted floodplain (Figure 4a). Background concentrations of Mn were substantially higher in the mine-impacted Coal Creek reach, and although channel sampling was more limited, large increases in concentration were observed over just a few hundred meters in the zone of return flows (Figure 5a). Plotting Fe vs Mn for all samples clearly demonstrates how return flows from beaver ponds dominate the anomalously high concentrations observed for both species, and although the ratio of the metals differed, Fe concentrations were almost always dominant (Figure 7c) consistent with Fe being preferentially elevated in comparison to Mn in the vast bulk of geologic materials. The mobility of As and Al was enhanced by beaver-induced floodplain exchanges (Figure 6e, f), as discussed in Section 3.3.

598 The spot DO measurements at East River beaver pond return flow
599seepages all showed varied degrees of suboxic condition (Figure 6a, Briggs
600et al., 2019a), though temporal redox fluctuations are not clear in these
601sparse sampling events. However, the redox potential profile collected
602directly within the return flow seep (shown flowing in Figure 3d) had
603systematic Eh shifts at all depths at daily to weekly timescales (Figure 7d).
604Overall there was a transition toward strong reducing conditions from June
60522 to July 11, 2018, except in the surface seepage pool where the probe was
606likely exposed to air periodically. The reducing shift likely results from the
607observed decreased seepage rates over time. Total flow from the seepage
608was physically measured to be 1464 L/d in late June but was too low to be
609reliably captured with the surface weir in late July, a reduction explained by
610the observed recession of the upgradient pond level during this period
611(decreased lateral hydraulic gradient). Vertical seepage rates measured over
61270 d in 2017 using iButton temperature sensors installed in this seep show
613coordinated short (daily) and longer-term flux patterns, also indicating that
614seepage redox chemistry (and associated metal concentrations) is likely to
615fluctuate over time (Figure 7a). As discussed in detail by Briggs et al. (2013),
616reactive mass flux beaver pond return seepages are not likely to occur at
617highest metal concentration but when fluid flux and concentration (typically
618inversely related) are optimally balanced. Therefore, higher flux surface
619return flows of lower metal concentration may be more important to river
620chemical dynamics than strongly reduced focused seepages. For example,

621the predominant East River return flow seepage transferred approximately
62210 g/d of dissolved Fe2+ to the main channel at times during this study,
623while the larger Coal Creek surface return flow transferred approximately
624218 g/d Fe2+.

625 In general, the focused return seepage water was less reduced toward
626the land surface along the redox profiler, indicating some vertical diffusive
627exchange with surface oxygen, and/or a convergence with oxic subsurface
628flowpaths at the seepage zone. During redox probe installation it was clear
629that beneath approximately 10 cm of fine sediments the focused seepage
630zone sediments were composed of higher permeability sands and gravels. As
631has been observed for numerous other river corridor seepage types, the
632distribution of spatially focused return flow seepages is likely controlled by
633existing heterogeneous floodplain geologic deposits where relatively coarse
634alluvium creates conduits of hydrologic exchange.

635 The areal ‘footprint’ of sub-oxic return flowpaths was mapped from the
636land surface using electromagnetic imaging. Higher frequencies of the GEM2
637tool should represent more shallow subsurface bulk EC dynamics, so raw
638data from the highest four frequencies (of 7 total frequencies) were
639arithmetically averaged for this analysis, as the lowest 3 frequencies were
640found to have reduced sensitivity in these systems. The resulting map of
641electrically-conductive subsurface anomalies below a larger beaver pond at
642the East River indicated a swath of reduced water 10’s of meters across

643flowing in the shallow subsurface toward the river, some of which discharges
644at the focused seep where the redox probe was installed (Figure 4c). These
645reactive flowpaths also source the diffuse seepage zones along the main
646channel margin, including the Fe-rich side channel shown in Figures 1d) and
647e). In general, electromagnetic imaging data collected throughout the
648channel area and over the opposite bank floodplain where there was no
649beaver activity did not indicate extensive subsurface plumes of metal-
650impacted water (Figure 4c). Vertical seepage rates along the channel margin
651were slow, typically less than 0.2 m d^{-1} over the 2017 period monitored with
652vertical iButtons (Figure 7a), but spatially extensive enough to drive the DO
653content of the side channel surface water down to an average of 54%
654saturation in mid-day during the summer 2018. Vertical seepage rates during
655the same period in 2017 for the focused beaver return flow seepage zone
656were stronger, ranging up to 0.6 m/d. Diffuse seepage rates at all 4 locations
657showed coordinated short-term shifts to downward flow, likely due to higher
658event flows in the channel. In contrast, discharge from the focused bank
659seep showed a different temporal pattern that is likely driven by beaver pond
660stage dynamics, and not directly impacted by channel flow.

661 A larger area was imaged along the Coal Creek, revealing 3 major ‘hot
662spots’ of increased shallow bulk EC (Figure 4b). The two upstream zones are
663adjacent to the main floodplain ponded areas in the vicinity of observed
664return flow seepages. This result agrees with the East River imaging, in that
665although seepages may be highly focused in space at the land surface, they

are fed and underlain by larger subsurface plumes of reduced metals. Of note, the downstream surface return flows, although enriched in Fe and Mn compared to channel water, do not create any extensive electromagnetic anomaly. This may be surprising given the extensive visible Fe staining along the creek sediments in this area (Figure 5c), but the GEM2 tool is sensitive to the upper several meters of earth material, and therefore this result indicates that the surficial return flows are not underlain by extensive subsurface reduced plumes. Much of the Fe oxides visible in this area may be precipitating from the nearby upstream highly reduced return flow subsurface seepages, and/or from the moderate concentrations of reduced Fe measured in the surface return flows. Further downstream, a channel spanning dam diverts channel water to both the right and left bank floodplain areas (Figure 5d). Flowpaths along the right bank appeared to stay on the land surface, remained oxic, and there was little enhancement of subsurface bulk EC. However, the downstream left floodplain area was highly reduced, mixing a valley wall groundwater seep with diverted channel water that returned to the stream in a series of seepages. Fe staining was prevalent in this area, and the floodplain pools and shallow subsurface highly electrically conductive (Figure 5b).

The main channel chemical time series (Fe, Mn, Al) were collected approximately 1 km downstream of each beaver-impacted reach (Figure 8). In total 299 samples were collected at the East River and 340 samples collected at Coal Creek over the 2017/2018 period. Main channel Fe

concentrations were typically measurable, indicating persistent inflow from reduced seepages. There was a bimodal pattern with early and late season peaks in concentration (over 50 ppb) at the East River that may be tied to the strong early and late season beaver-induced floodplain connection mentioned above (Figure 8a). Mn was generally quite low or below the detection limit, except for a few spikes coinciding with Fe highs. When East River Fe and Al are plotted against each other there is no strong proportional relation (Figure 8b), indicating other processes in addition to reduced return flows drive Al concentration dynamics. This may be explained in part by the high concentrations of Al observed at the floodplain valley wall geologic groundwater seepages, such that some combination of groundwater discharge and beaver-induced floodplain exchange influences downstream Al concentration. A bimodal temporal pattern of main channel Fe concentration was also observed at Coal Creek (Figure 8c), where Mn concentrations were generally much higher than at East River and better coupled with Fe. A strong proportional relation was observed between Fe and Al at Coal Creek indicating that for that system reduced return flow seepages may drive Al mobility (Figure 8d). Unlike the East River, Al concentration in the local Coal Creek beaver-impacted reach hillslope groundwater was low, based on limited data.

3.3 Metal oxide deposition at beaver pond return flows

Oxides and hydroxides (referred to here by the general term “oxides”) of Mn and Fe metals are often associated with groundwater seepage zones

(Boano et al., 2014; Gandy et al., 2007) and characteristic red staining of surface sediments is frequently used to visually locate points of sub-oxic seepage (e.g. Figure 1e; Figure 5c,d). Similar to engineered geochemical barriers using zero-valent Fe (McCobb et al., 2018), metal oxides function as a sorption sink for a host of dissolved contaminants toxic to humans and aquatic life. In watersheds, such as Coal Creek that are impacted by mine water drainage, Mn oxides have been shown to sorb and co-precipitate cobalt, nickel, and zinc in high concentrations (Jenne, 1968). Fe oxides have also been shown to substantially reduce these contaminants as groundwater flows through the streambed, and to be a strong sink for arsenic (Nagorski and Moore, 1999). In zones of uranium contamination, adsorption to biogenic Fe oxides can strip hexavalent uranium (U(VI)) from groundwater (Katsoyiannis, 2007) before discharge to surface water. Fe oxides have also been shown as important sorption sites for perfluorooctane sulfonate (PFOS) (Johnson et al., 2007), a contaminant of major emerging concern (Banzhaf et al., 2016). However, dynamic dissolution of oxides under dynamic reducing conditions of beaver-impacted floodplain soils can mobilize previously sequestered contaminants along with the dissolved metals.

Along the river corridor, solid grain Fe and Mn is typically found in glacial sediment grains, alluvial sediments, and mine tailings. Reduction to soluble form under suboxic condition mobilizes the metals to travel with hyporheic flow, groundwater, or as this study has shown, in surface return flows and subsurface seepages. Widespread Fe staining below return flow

discharge points along the East River and Coal Creek corridors visibly indicates how beaver activity can greatly alter metal oxide dynamics in alluvial systems (Figure 5c, d). For example, a side channel along the East River adjacent to the return seepages that was instrumented with iButtons and the redox probe, was shown to collect reduced water loaded with natural metals (Figure 1e), and precipitate oxides as this water exchanged gas with air and advectively mixed with the main channel.

Arsenic and aluminum concentrations were predominantly higher in the mine-impacted Coal Creek return flow samples as compared to the East River, averaging 6.3 and 10.1 µg/L, respectively. These concentrations are approximately 2x higher than that observed in the diverted channel water, suggesting the mobility of these contaminants is tied to the dissolution of floodplain metal oxides. Considering the importance of metal oxides to a host of abiotic and biotic processes, beaver pond return flows of reduced water could be recognized as ecosystem control points (Bernhardt et al., 2017), and deserve similar research attention to more commonly studied mechanisms of river to floodplain hydrologic exchange. Several western USA alluvial river corridors with similar morphology to East River have contemporary U(VI) contamination concerns resulting from legacy floodplain mine tailings (Curtis et al., 2006; Naftz et al., 2018), and it has been shown that mobility of U(VI) is directly tied to Fe oxide dynamics in NRZs (Bone et al., 2017; Davis et al., 2006). In such systems the return of beaver, or human

simulation of their dam construction using dam analogues, may result in undesirable transport of contaminants.

4. Conclusions

Enhanced river/floodplain hydrologic connection has been shown to increase river corridor evapotranspiration and net carbon uptake (Missik et al., 2018), but the impact of beaver-induced floodplain water flux on the mobility of river corridor metals has been largely under-characterized. In the two alluvial systems studied here, we observed high-flow active shunting of stream water onto adjacent floodplains, greatly expanding the volume of saturated floodplain sediments with strong hydrologic connectivity to the channel. Land surface and subsurface beaver pond return flows contained high concentrations of dissolved Mn and Fe, redox-sensitive metals that are highly influential to a multitude of biogeochemical and abiotic processes. Dissolution of solid phase floodplain sediment Mn and Fe oxides can provide an advective pathway for contaminant transport, particularly in mine-impacted watersheds. In contrast to episodic overbank river flow events or slower-exchanging meander bend flowpaths, beaver-induced exchanges can provide strong, persistent river-floodplain connectivity and conduits for metal mobility. As beaver return to alluvial floodplain systems across north America, active human management will likely need to consider system-specific consequences of enhanced exchange with suboxic floodplain waters,

778to be balanced against numerous desirable hydroecological and restorative
779outcomes.

Acknowledgments

Funding for this methods development was provided by U.S. Department of Energy grant DE-SC0016412 and the U.S. Geological Survey (USGS) Toxic Substances Hydrology Program. This material is partially based upon work supported through the Lawrence Berkeley National Laboratory's Watershed Function Scientific Focus Area. The U.S. Department of Energy (DOE), Office of Science, Office of Biological and Environmental Research, Subsurface Biogeochemical Research Program funded the work under contract DE-AC02-05CH11231 (Lawrence Berkeley National Laboratory; operated by the University of California). We thank Jennifer Reithel and the Rocky Mountain Biological Laboratory for logistical support; Lee Slater, Dylan Fosberg, Kimberly Moore, Cian Dawson, Eric White, Josip Adams, Christopher Holmquist-Johnson, Jalise Wright, and Bianca Isabelle Abrera for field data collection; Rosemary Carroll for providing the HUC boundaries used in Figure 1; Mike Wilkins and other anonymous reviewers for peer review early drafts. Any use of trade, firm, or product names is for descriptive purposes only and does not imply endorsement by the U.S. Government.

37

References

Bailey, D.R., Dittbrenner, B.J., Yocom, K.P., 2019. Reintegrating the North American beaver (Castor canadensis) in the urban landscape. WIREs Water 6. https://doi.org/10.1002/wat2.1323

Banzhaf, S., Sparrenbom, C.J., Banzhaf, S., Filipovic, M., Lewis, J., Sparrenbom, C.J., Barthel, R., 2016. A review of contamination of surface-, ground- , and drinking water in Sweden by perfluoroalkyl and polyfluoroalkyl ... Ambio. https://doi.org/10.1007/s13280-016-0848-8

Boano, F., Demaria, A., Revelli, R., Ridolfi, L., 2010. Biogeochemical zonation due to intrameander hyporheic flow. Water Resour. Res. 46, W02511. https://doi.org/10.1029/2008wr007583

Boano, F., Harvey, J.W., Marion, A., Packman, A.I., Revelli, R., Ridolfi, L., Worman, A., 2014. Hyporheic flow and transport processes: Mechanisms, models, and biogeochemical implications. Rev. Geophys. 1–77. https://doi.org/10.1002/2012RG000417.Received

Bone, S.E., Cahill, M.R., Jones, M.E., Fendorf, S., Davis, J., Williams, K.H., Bargar, J.R., 2017. Oxidative Uranium Release from Anoxic Sediments under Diffusion- Limited Conditions. Environ. Sci. Technol. 51, 11039–11047. https://doi.org/10.1021/acs.est.7b02241

38

Bouwes, N., Weber, N., Jordan, C.E., Saunders, W.C., Tattam, I.A., Volk, C., Wheaton, J.M., Pollock, M.M., 2016. Ecosystem experiment reveals benefits of natural and simulated beaver dams to a threatened population of steelhead (Oncorhynchus mykiss). Nat. Sci. Reports 1–13. https://doi.org/10.1038/srep28581

Boye, K., Noël, V., Tfaily, M.M., Bone, S.E., Williams, K.H., Bargar, J.R., Fendorf, S., 2017. Thermodynamically controlled preservation of organic carbon in floodplains. Nat. Geosci. 10, 415–419. https://doi.org/10.1038/NGEO2940

Briggs, M.A., Chen, W., Slater, L.D., Day-Lewis, F.D., 2019a. Hydrogeochemical data for the characterization of stream, groundwater, and beaver-induced floodplain exchange in the East River Science Focus Area, Crested Butte, CO. U.S. Geol. Surv. Data Release. https://doi.org/10.5066/P9Q1Z1TK

Briggs, M.A., Dawson, C.B., Holmquist-Johnson, C.L., Williams, K.H., Lane, J.W., 2019. Efficient hydrogeological characterization of remote stream corridors using drones. Hydrol. Process. 33. https://doi.org/10.1002/hyp.13332

Briggs, M.A., Dawson, C.B., White, E.A., Holmquist-Johnson, C.L., 2019b. Thermal infrared, multispectral, and photogrammetric data collected by drone for hydrogeologic analysis of the East River and Coal Creek beaver-impacted corridors near Crested Butte, Colorado. U.S. Geol. Surv.

Data Release. https://doi.org/10.5066/P9YWSJ2J

Briggs, M.A., Lautz, L.K., Buckley, S.F., Lane, J.W., 2014. Practical limitations on the use of diurnal temperature signals to quantify groundwater upwelling. J. Hydrol. 519, 1739–1751. https://doi.org/10.1016/j.jhydrol.2014.09.030

Briggs, M.A., Lautz, L.K., Hare, D.K., González-Pinzón, R., 2013. Relating hyporheic fluxes, residence times, and redox-sensitive biogeochemical processes upstream of beaver dams. Freshw. Sci. 32, 622–641. https://doi.org/10.1899/12-110.1

Burchsted, D., Daniels, M., Thorson, R., Vokoun, J., 2010. The River Discontinuum: Applying Beaver Modifications to Baseline Conditions for Restoration of Forested Headwaters. Bioscience 60, 908–922. https://doi.org/10.1525/bio.2010.60.11.7

Catalán, N., Herrero Ortega, S., Gröntoft, H., Hilmarsson, T.G., Bertilsson, S., Wu, P., Levanoni, O., Bishop, K., Bravo, A.G., 2017. Effects of beaver impoundments on dissolved organic matter quality and biodegradability in boreal riverine systems. Hydrobiologia 793, 135–148. https://doi.org/10.1007/s10750-016-2766-y

Cirmo, C.P., Driscoll, C.T., 1993. Beaver pond biogeochemistry: Acid neutralizing capacity generation in a headwater wetland. Wetlands 13, 277–292.

865Collen, P., Gibson, R.J., 2000. The general ecology of beavers (Castor spp.),
866 as related to their influence on stream ecosystems and riparian habitats,
867 and the subsequent effects on fish - A review. Rev. Fish Biol. Fish. 10,
868 439–461. https://doi.org/10.1023/A:1012262217012

869Constantz, J., 2008. Heat as a tracer to determine streambed water
870 exchanges. Water Resour. Res. 44, 1–20.
871 https://doi.org/10.1029/2008WR006996

872Covino, T., 2017. Hydrologic connectivity as a framework for understanding
873 biogeochemical flux through watersheds and along fluvial networks.
874 Geomorphology 277, 133–144.
875 https://doi.org/10.1016/j.geomorph.2016.09.030

876Curtis, G.P., Davis, J. a., Naftz, D.L., 2006. Simulation of reactive transport of
877 uranium(VI) in groundwater with variable chemical conditions. Water
878 Resour. Res. 42, 1–15. https://doi.org/10.1029/2005WR003979

879Davis, J.A., Curtis, G.P., Wilkins, M.J., Kohler, M., Fox, P., Naftz, D.L., Lloyd,
880 J.R., 2006. Processes affecting transport of uranium in a suboxic aquifer.
881 Phys. Chem. Earth, Parts A/B/C 31, 548–555.
882 https://doi.org/10.1016/j.pce.2006.04.005

883Dugdale, S.J., 2016. A practitioner’s guide to thermal infrared remote sensing
884 of rivers and streams: recent advances, precautions and considerations.
885 WIREs Water. https://doi.org/10.1002/wat2.1135

886Dwivedi, D., Arora, B., Steefel, C.I., Dafflon, B., Versteeg, R., 2018. Hot Spots
887 and Hot Moments of Nitrogen in a Riparian Corridor. Water Resour. Res.
888 54, 205–222. https://doi.org/10.1002/2017WR022346

889Essaid, H.I., Caldwell, R.R., 2017. Science of the Total Environment
890 Evaluating the impact of irrigation on surface water – groundwater
891 interaction and stream temperature in an agricultural watershed. Sci.
892 Total Environ. 599–600, 581–596.
893 https://doi.org/10.1016/j.scitotenv.2017.04.205

894Gandy, C.J., Smith, J.W.N., Jarvis, A.P., 2007. Attenuation of mining-derived
895 pollutants in the hyporheic zone : A review. Sci. Total Environ. 373, 435–
896 446. https://doi.org/10.1016/j.scitotenv.2006.11.004

897Handcock, R.N., Gillespie, a. R., Cherkauer, K. a., Kay, J.E., Burges, S.J.,
898 Kampf, S.K., 2006. Accuracy and uncertainty of thermal-infrared remote
899 sensing of stream temperatures at multiple spatial scales. Remote Sens.
900 Environ. 100, 427–440. https://doi.org/10.1016/j.rse.2005.07.007

901Hare, D.K., Briggs, M.A., Rosenberry, D.O., Boutt, D.F., Lane, J.W., 2015. A
902 comparison of thermal infrared to fiber-optic distributed temperature
903 sensing for evaluation of groundwater discharge to surface water. J.
904 Hydrol. 530, 153–166. https://doi.org/10.1016/j.jhydrol.2015.09.059

905Harvey, J.W., Gooseff, M.N., 2015. River corridor science: Hydrologic
906 exchange and ecological consequences from bedforms to basins. Water

907 Resour. Res. 51, 1–30. https://doi.org/10.1002/2015WR017617.Received

908Hood, G., 2011. The Beaver Manifesto. Rocky Mountian Books, Calgary, CAN.

909Hood, G.A., Bayley, S.E., 2008. Beaver (Castor canadensis) mitigate the
910 effects of climate on the area of open water in boreal wetlands in
911 western Canada. Biol. Conserv. 141, 556–567.
912 https://doi.org/10.1016/j.biocon.2007.12.003

913Irvine, D.J., Briggs, M.A., Cartwright, I., Scruggs, C.R., Lautz, L.K., 2017.
914 Improved Vertical Streambed Flux Estimation Using Multiple Diurnal
915 Temperature Methods in Series. Groundwater 55.
916 https://doi.org/10.1111/gwat.12436

917Irvine, D.J., Lautz, L.K., Briggs, M.A., Gordon, R.P., Mckenzie, J.M., 2015.
918 Experimental evaluation of the applicability of phase, amplitude, and
919 combined methods to determine water flux and thermal diffusivity from
920 temperature time series using VFLUX 2. J. Hydrol. 531, 728–737.

921Janot, N., Lezama Pacheco, J.S., Pham, D.Q., O'Brien, T.M., Hausladen, D.,
922 Noël, V., Lallier, F., Maher, K., Fendorf, S., Williams, K.H., Long, P.E.,
923 Bargar, J.R., 2016. Physico-Chemical Heterogeneity of Organic-Rich
924 Sediments in the Rifle Aquifer, CO: Impact on Uranium Biogeochemistry.
925 Environ. Sci. Technol. 50, 46–53. https://doi.org/10.1021/acs.est.5b03208

926Jenne, E.A., 1968. Chapter 21: Controls on Mn, Fe, Co, Ni, Cu, and Zn
927 concentrations in soils and water: the significant role of hydrous Mn and

928 Fe oxides, in: Trace Inorganics in Water. American Chemical Society, pp.
929 337–387. https://doi.org/10.1021/ba-1968-0073.ch021

930Jin, L., Siegel, D.I., Lautz, L.K., Otz, M.H., 2009. Transient storage and
931 downstream solute transport in nested stream reaches affected by
932 beaver dams. Hydrol. Process. 23, 2438–2449. https://doi.org/Cited By
933 (since 1996) 1Export Date 4 April 2012

934Johnson, R.L., Anschutz, A.J., Smolen, J.M., Simcik, M.F., Penn, R.L., 2007. The
935 Adsorption of Perfluorooctane Sulfonate onto Sand, Clay, and Iron Oxide
936 Surfaces. J. Chem. Eng. Data 52, 1165–1170.
937 https://doi.org/10.1021/je060285g

938Katsoyiannis, I.A., 2007. Carbonate effects and pH-dependence of uranium
939 sorption onto bacteriogenic iron oxides : Kinetic and equilibrium studies.
940 J. Hazard. Mater. 139, 31–37.
941 https://doi.org/10.1016/j.jhazmat.2006.05.102

942Lautz, L., Kelleher, C., Vidon, P., Coffman, J., Riginos, C., Copeland, H., 2018.
943 Restoring stream ecosystem function with beaver dam analogues: Let’s
944 not make the same mistake twice. Hydrol. Process. 174–177.
945 https://doi.org/10.1002/hyp.13333

946Ligon, F.K., Dietrich, W.E., Trush, W.J., 1995. Downstream Ecological Effects
947 of Dams. Bioscience 45, 183–192. https://doi.org/10.2307/1312557

948Luce, C.H., Tonina, D., Gariglio, F., Applebee, R., 2013. Solutions for the

diurnally forced advection-diffusion equation to estimate bulk fluid velocity and diffusivity in streambeds from temperature time series. Water Resour. Res. 49, 488–506. https://doi.org/10.1029/2012WR012380

Majerova, M., Neilson, B.T., Schmadel, N.M., Wheaton, J.M., Snow, C.J., 2015. Impacts of beaver dams on hydrologic and temperature regimes in a mountain stream. Hydrol. Earth Syst. Sci. 3541–3556. https://doi.org/10.5194/hess-19-3541-2015

McCobb, T.D., Briggs, M.A., LeBlanc, D.R., Day-Lewis, F.D., Johnson, C.D., 2018. Evaluating long-term patterns of decreasing groundwater discharge through a lake-bottom permeable reactive barrier. J. Environ. Manage. 220, 233–345. https://doi.org/10.1016/j.jenvman.2018.02.083

Missik, J.E.C., Liu, H., Gao, Z., Huang, M., Chen, X., Arntzen, E., Mcfarland, D.P., Ren, H., Titzler, P.S., Jonathan, N., 2018. Groundwater - river water exchange enhances growing season evapotranspiration and carbon uptake in a semi - arid riparian ecosystem. https://doi.org/10.1029/2018JG004666

Naftz, D.L., Fuller, C.C., Runkel, R.L., Briggs, M.A., Solder, J.E., Cain, D.J., Short, T.M., Gardner, P.M., Byrne, P., Terry, N., Gobel, D., 2018. Hydrologic, biogeochemical, and radon data collected within and adjacent to the Little Wind River near Riverton, Wyoming. US Geol. Surv. Data Release.

970Nagorski, S.A., Moore, J.N., 1999. Arsenic mobilization in the hyporheic zone
971 of a stream 35, 3441–3450.

972Naiman, R.J., Johnston, C.A., Kelley, J.C., 1988. Alteration of North American
973 Streams by Beaver. Bioscience 38, 753–762.
974 https://doi.org/10.2307/1310784

975Naiman, R.J., Melillo, J.M., Hobbie, J.E., 1986. Ecosystem alteration of boreal
976 forest streams by beaver (Castor canadensis). Ecology 67, 1254–1269.

977Nash, C.S., Selker, J.S., Grant, G.E., Lewis, S.L., Noël, P., 2018. A physical
978 framework for evaluating net effects of wet meadow restoration on late -
979 summer streamflow. Ecohydrology 1–15.
980 https://doi.org/10.1002/eco.1953

981Pai, H., Malenda, H.F., Briggs, M.A., Singha, K., González-Pinzón, R., Gooseff,
982 M.N., Tyler, S.W., 2017. Potential for Small Unmanned Aircraft Systems
983 Applications for Identifying Groundwater-Surface Water Exchange in a
984 Meandering River Reach. Geophys. Res. Lett. 44.
985 https://doi.org/10.1002/2017GL075836

986Pilliod, D.S., Rohde, A.T., Charnley, S., Davee, R.R., Dunham, J.B., Gosnell, H.,
987 Grant, G.E., Hausner, M.B., Huntington, J.L., Nash, C., 2018. Survey of
988 Beaver-related Restoration Practices in Rangeland Streams of the
989 Western USA. Environ. Manage. 61, 58–68.
990 https://doi.org/10.1007/s00267-017-0957-6

991Poole, G.C., 2010. Stream hydrogeomorphology as a physical science basis
992 for advances in stream ecology. J. N. Am. Benthol. Soc 29, 12–25.
993 https://doi.org/10.1899/08-070.1

994Sawyer, A.H., Kaplan, L.A., Lazareva, O., Michael, H.A., 2014. Hydrologic
995 dynamics and geochemical responses within a floodplain aquifer and
996 hyporheic zone during Hurricane Sandy. Water Resour. Res. 50, 4877–
997 4892. https://doi.org/10.1002/2013WR015101.Received

998Schulz-Zunkel, C., Krueger, F., 2009. Trace Metal Dynamics in Floodplain
999 Soils of the River Elbe : A Review. J. Environ. Qual. 38, 1349–1362.
1000 https://doi.org/10.2134/jeq2008.0299

1001Seton E.T., 1929. Lives of Game Animals. Doubleday, Doran & Co., Garden
1002 City N.Y.

1003Tyler, S.W., Selker, J.S., Hausner, M.B., Hatch, C.E., Torgersen, T., Thodal,
1004 C.E., Schladow, S.G., 2009. Environmental temperature sensing using
1005 Raman spectra DTS fiber-optic methods. Water Resour. Res. 45, 1–11.
1006 https://doi.org/10.1029/2008WR007052

1007US Geological Survey, 2011. Change to solubility equations for oxygen in
1008 water: Office of Water Quality Technical Memorandum 2011.03.
1009 https://doi.org//admin/memo/QW/qw11.03.pdf

1010Vidon, P., Allan, C., Burns, D., Duval, T.P., Gurwick, N., Inamdar, S., Lowrance,
1011 R., Okay, J., Scott, D., Sebestyen, S., Allan, C., Burns, D., Duval, T.P.,

1012 Gurwick, N., Inamdar, S., Low-, R., 2010. Hot spots and hot moments in
1013 riparian zones: potential for improved water quality management. J. Am.
1014 water Resour. Assoc. 46, 278–298.

1015 Weber, N., Bouwes, N., Pollock, M.M., Volk, C., Wheaton, M., Wathen, G.,
1016 Wirtz, J., Jordan, C.E., 2017. Alteration of stream temperature by natural
1017 and artificial beaver dams. PLoSONE 12, 1–23.
1018 https://doi.org/10.17605/OSF.IO/6MMGZ.Funding

1019 Wegener, P., Covino, T.P., Wohl, E.E., 2017. Beaver-mediated lateral
1020 hydrologic connectivity, fluvial carbon and nutrient flux, and aquatic
1021 ecosystemmetabolism. Water Resour. Res. 53, 4606–4623.
1022 https://doi.org/10.1002/2016WR019538.Received

1023 Westbrook, C.J., Cooper, D.J., Baker, B.W., 2006. Beaver dams and overbank
1024 floods influence groundwater-surface water interactions of a Rocky
1025 Mountain riparian area. Water Resour. Res. 42, 1–12.
1026 https://doi.org/10.1029/2005WR004560

1027 Williams, K.H., 2019. Geochemical data from the East River Science Focus
1028 Area. DOE public data release.

1029 Winter, T.C., Harvey, J.W., Franke, O.L., Alley, W.M., 1998. Ground water and
1030 surface water; a single resource. U . S . Geol. Surv. Circ. 1139 79.

1031 Wohl, E.E., Lane, S.N., Wilcox, A.C., 2015. The science and practice of river
1032 restoration. Water Resour. Res. 51, 5974–5997. https://doi.org/10.1002/

1033 2014WR016874

1034 Wondzell, S.M., 2011. The role of the hyporheic zone across stream
1035 networks. Hydrol. Process. 25, 3525–3532.
1036 https://doi.org/10.1002/hyp.8119

1037 Young, P.C., Taylor, C.J., Tych, W., Pegregal, D.J., McKenna, P.G., 2010. The
1038 Captain Toolbox, Centre for Research on Environmental Systems and
1039 Statistics, Lancaster University. UK.

1040 Zarnetske, J.P., Haggerty, R., Wondzell, S.M., Bokil, V.A., González-Pinzón, R.,
1041 2012. Coupled transport and reaction kinetics control the nitrate source-
1042 sink function of hyporheic zones. Water Resour. Res. 48, W11508.
1043 https://doi.org/10.1029/2012WR011894

1044

1045 **Graphical Abstract**

1046 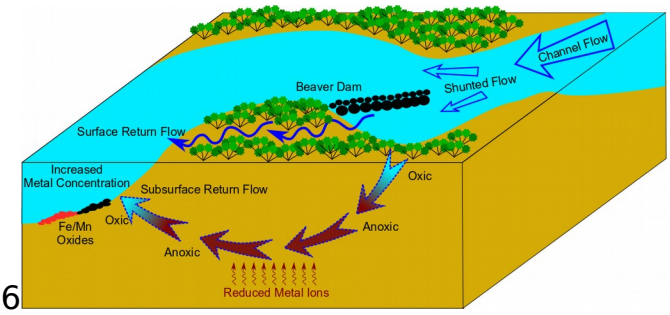

Figures

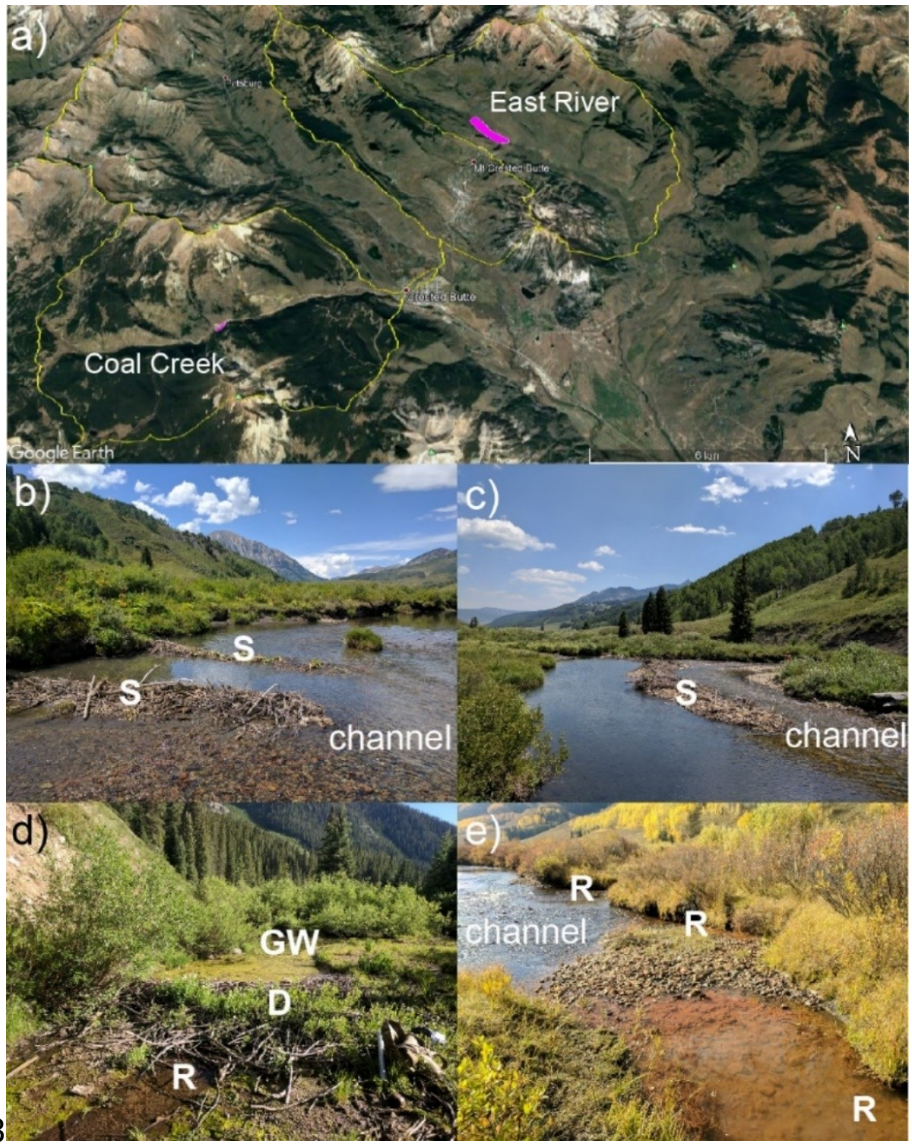

Figure 1. Pane1 a) shows the sub-watersheds of the East River SFA, where the Coal Creek and East River beaver-impacted study floodplain sections are highlighted in pink. In spring and summer, beavers construct a series of dams at the East River to ‘shunt’ (S) large volumes of channel water onto the adjacent floodplain (panels b,c). Discrete hillslope groundwater (GW) springs may be directly captured by small beaver dams (D) (panel d) before draining

to the main channel, while beaver pond return flow seeps (R) are typically warmer and lower in oxygen in summer (panel e).

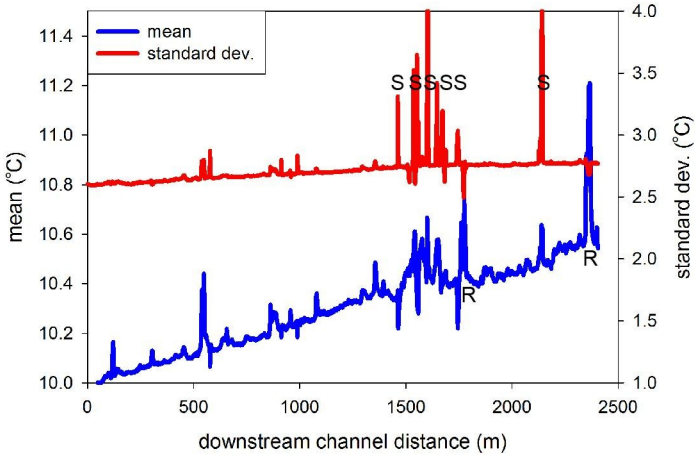

Figure 2. The 6-day mean and standard deviation of temperature along the East River fiber-optic cable showing influence of ‘shunt’ beaver dam construction (S) and shallow, warm beaver pond return flow seepage (R).

51

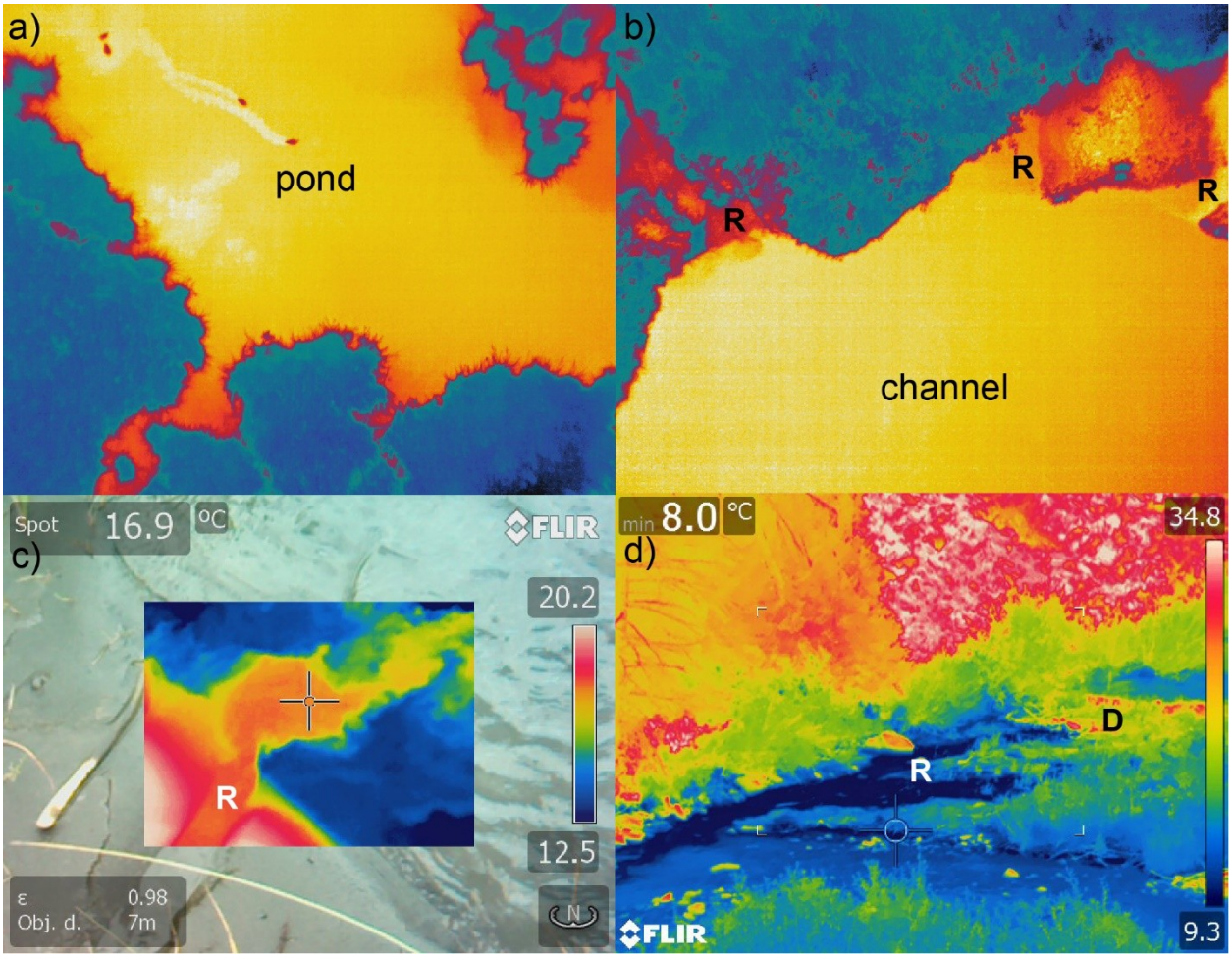

1062

1063Figure 3. Thermal infrared imaging collected by drone of floodplain beaver

1064ponds show relatively warm ponded areas, indicating by the hot colors in

1065panel a), and beaver pond return flow seepage is shown by relative color

1066scale in panel b), and close up through handheld imaging in panel c).

1067Hillslope springs captured by floodplain beaver ponds collect relatively cold,

1068deeper groundwater that discharges to the main channel after mixing with

1069floodplain water (panel (d)).

1070

52

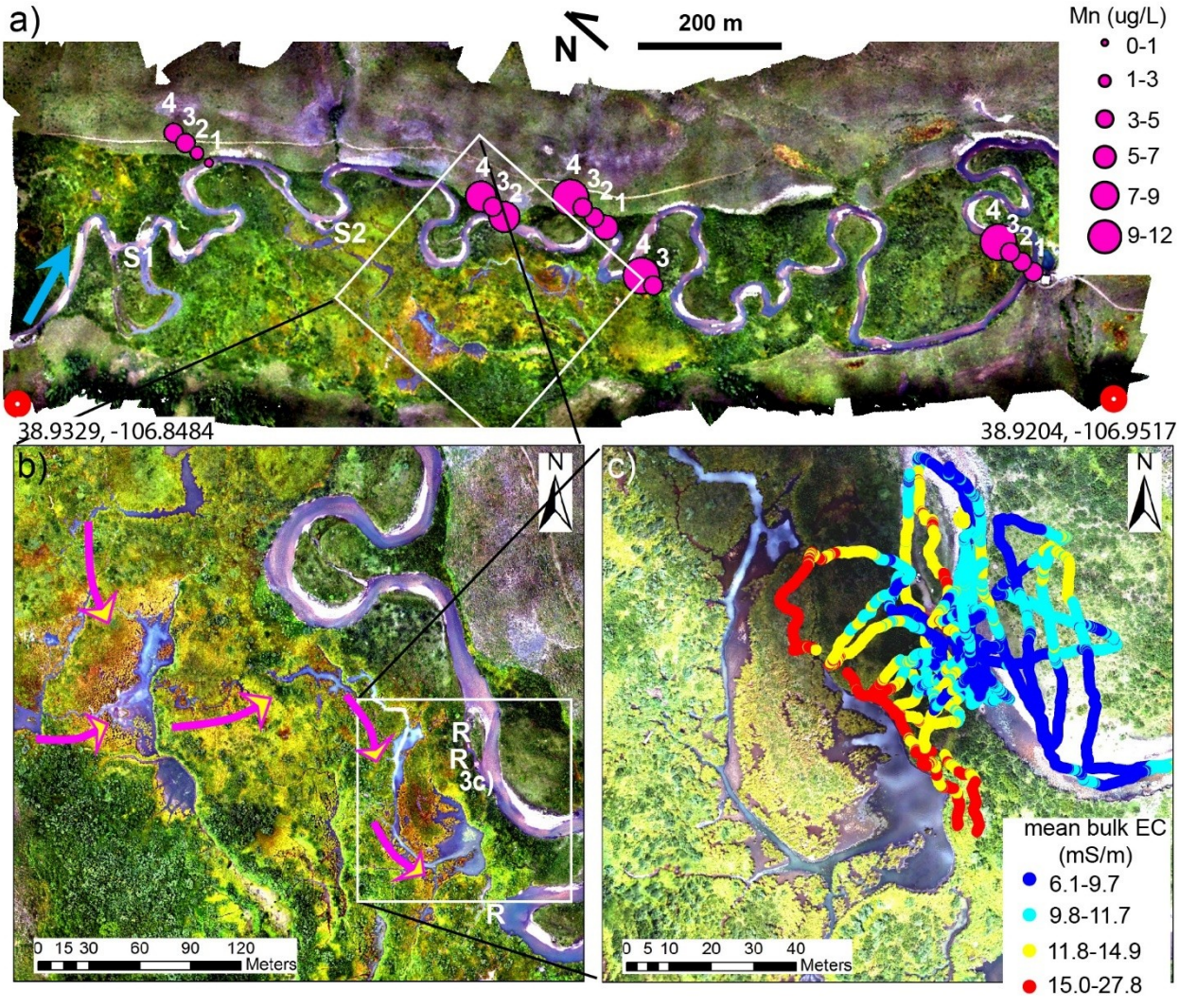

1071

1072Figure 4. Panel a) displays the full size orthomosaic generated from 2017
1073drone imagery collected along the East River beaver impacted reach (north
1074direction rotated left). River flow is left to right, and the two main beaver
1075shunts are marked (S1, S2) that push channel water onto the adjacent
1076floodplain. Main river channel dissolved manganese concentrations are
1077shown for samples collected on: 1. August 2017, 2. June 21, 2018, 3. July 30,
10782018, and 4. September 23, 2018. Panel b) shows an enlarged image of the
10792017 imagery of the more prominent floodplain beaver ponds and major

return flow seeps (R), including the approximate location of the infrared image of Figure 3c). General surface flow patterns are shown with yellow arrowheads as inferred from fine, light colored sediment transport following a rain event. Panel c) is an enlarged image of the 2018 drone-based orthomosaic showing lower pond water levels. Electromagnetic imaging transects indicate shallow subsurface plumes of reduced water (higher bulk conductivity) extending from the ponded area toward the main channel.

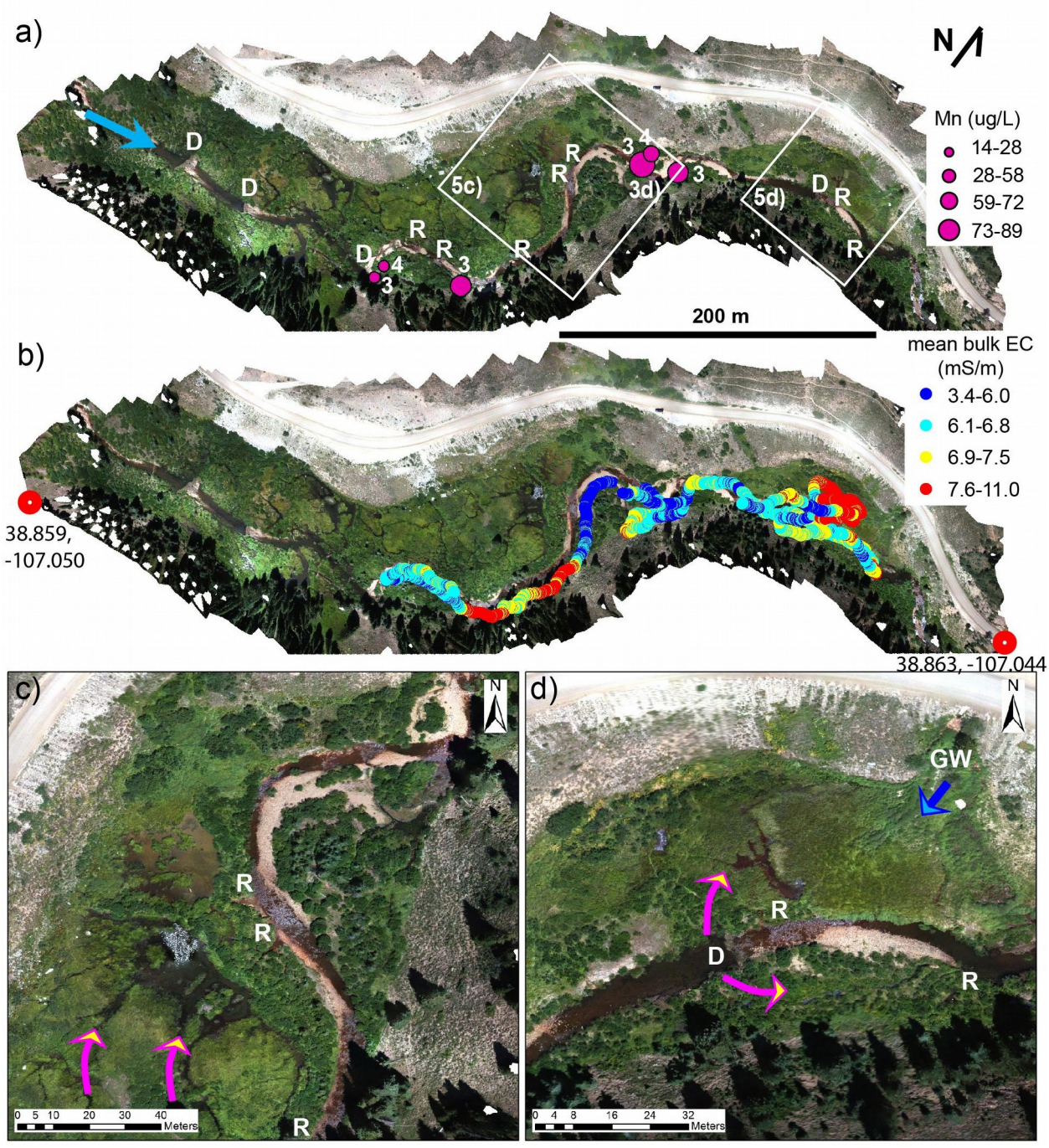

1087

1088Figure 5. Panel a) shows the full orthomosaic generated from 2018 drone

1089imaging collected along the Coal Creek beaver impacted reach. Stream flow

1090is left to right and channel spanning beaver dams (D), return flows (R), and

1091the locations of Figure panels 3d), 5c), and 5d) are marked. Main channel

55

dissolved manganese concentrations are shown for two sampling events on: 3. August 2, 2018, and 4. September 25, 2018. Panel b) covers the same spatial extent as a), and shows electromagnetic imaging transects data. Panel c) displays an enlarged view of the larger floodplain ponds, and Panel d) shows a zoomed view of the most downstream channel spanning dam and resulting floodplain diversions.

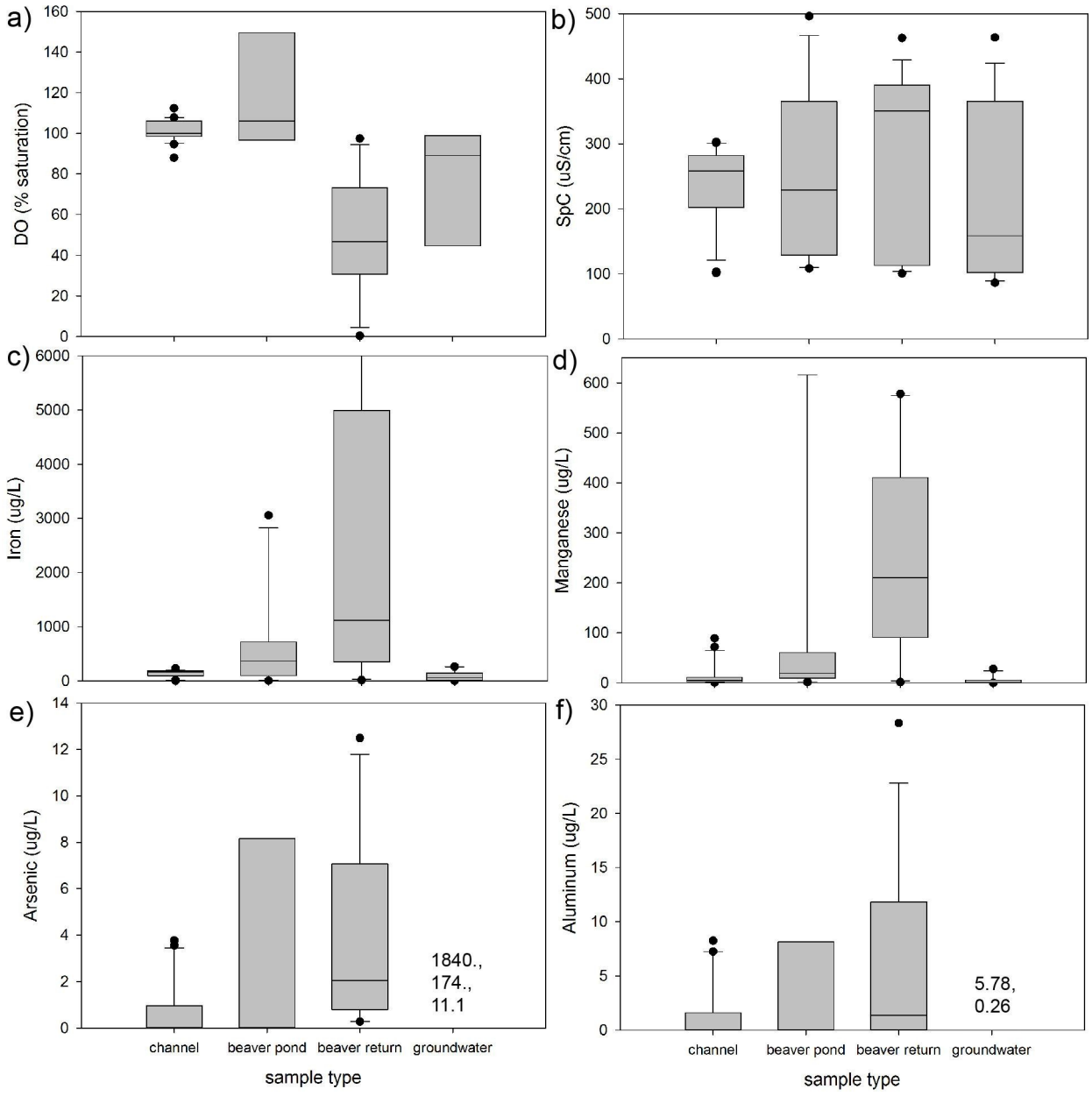

1099

1100Figure 6. Water samples of source type: a) dissolved oxygen, b) specific

1101conductivity, c) iron, d) manganese, e) arsenic, and f) aluminum. The vertical

1102box indicates the interquartile range and the dots are outliers. For plots e)

1103and f) all groundwater samples were below the respective detection limits

1104except for the discrete values listed. The full chemical dataset is listed by

1105sample in the Supplemental Material.

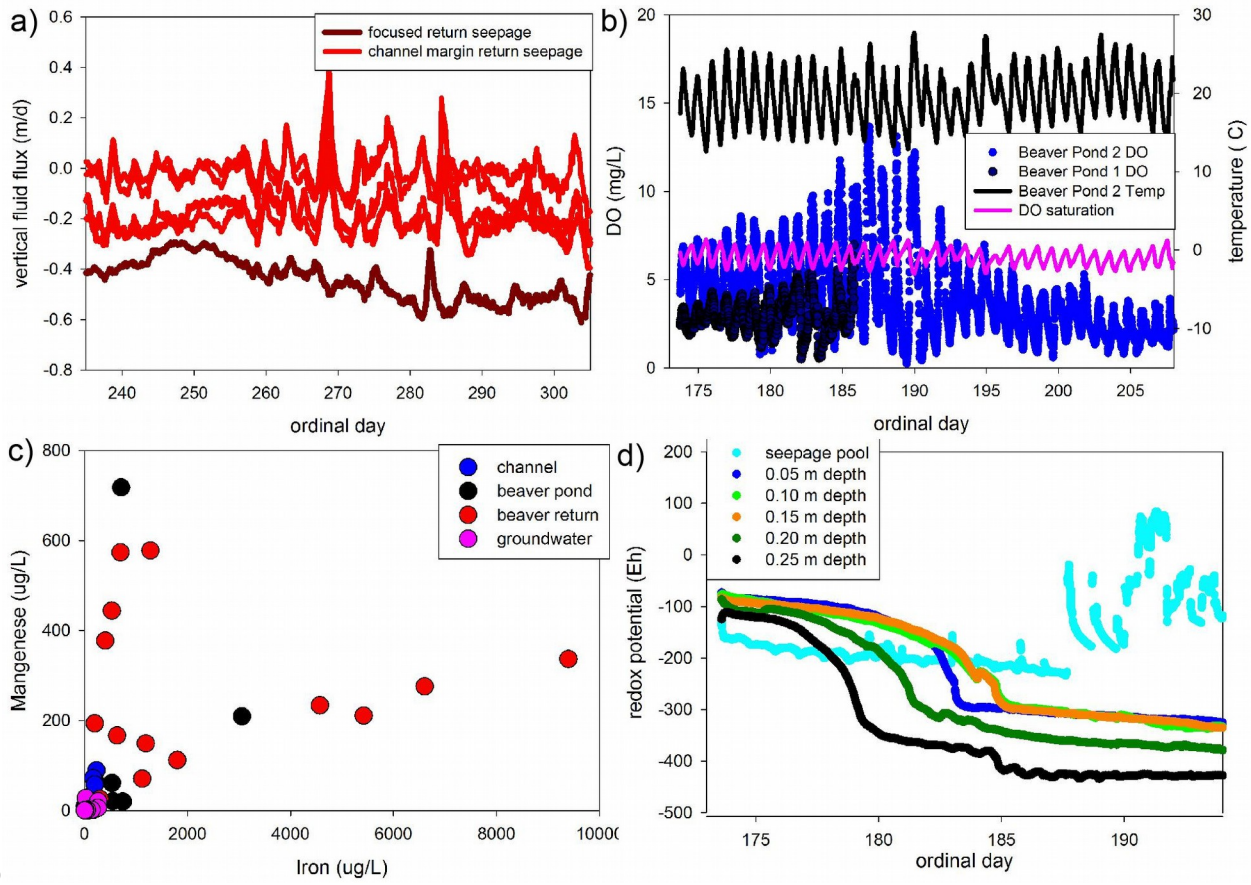

1106

1107Figure 7. Panel a) displays summer/fall 2017 vertical return flow seepage
1108rates, while panel b) shows measured dissolved oxygen (DO), temperature,
1109and theoretical oxygen saturation for East River beaver ponds. Panel c)
1110shows a plot of dissolved iron vs. manganese for all water samples of varied
1111type; a sample of 14260.0 µg/L Fe and 472.5 µg/L Mn collected at the same
1112location of the redox profile is not displayed. Panel d) displays multi-depth
1113redox potential (Eh) monitored directly at the discharge point over time at a
1114major East River return flow seep (shown in Figure 3b).

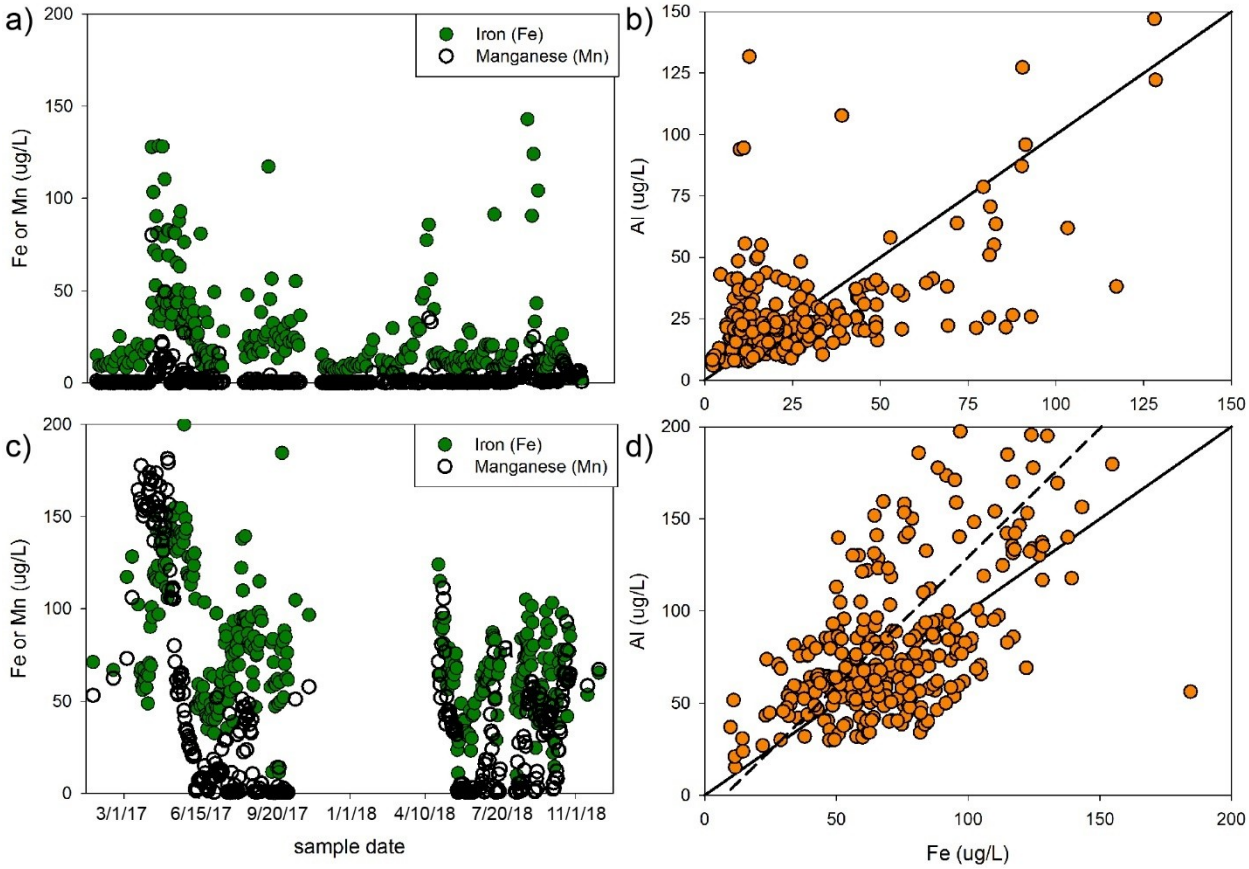

1115

1116Figure 8. Time series of iron, manganese, and aluminum collected over 2017-
11172018 1 km downstream of the distal end of the East River (panels a,b) and
1118Coal Creek (panels b,c) beaver-impacted reaches. The solid line in panels b)
1119and d) indicates a 1:1 relation while the dashed line in panel d) indicates the
1120best linear fit to the data (R^2=0.52), no significant linear relation was found
1121for the data in panel b).